Chem Soc Rev

REVIEW ARTICLE

Synthesis of new zeolite structures

Jiyang Li,[a] Avelino Corma[b] and Jihong Yu*[a]

Cite this: *Chem. Soc. Rev.*, 2015, **44**, 7112

Received 11th January 2015

DOI: 10.1039/c5cs00023h

www.rsc.org/csr

The search for new zeolites is of continuous interest in the field of zeolite science because of their widespread application in catalysis and adsorption–separation. To this end, considerable efforts have been devoted to the preparation of new zeolites with novel porous architectures and compositions. Taking account of the key factors governing the formation of zeolites (*e.g.*, guest species, framework elements, construction processes, *etc.*), several synthetic strategies have been developed recently. These allow the discovery of many new zeolites with unprecedented structural features, such as hierarchical pores, odd-ring numbers (11-, 15-rings), extra-large pores (16-, 18-, 20-, 28-, and 30-rings), chiral pores, and extremely complex framework topologies, *etc.* In this review, we will present the advances in the synthesis of new zeolite structures in the last decade, which are achieved by utilization of the synthetic strategies based on pre-designed structure-directing agents, heteroatom substitution, and topotactic transformations.

1. Introduction

Zeolites, as a class of inorganic microporous crystalline materials, are widely used in catalysis, adsorption–separation, and ion-exchange.[1] In addition, new applications of zeolitic materials have also been found in luminescence, electricity, magnetism, medicine, and microelectronics, *etc.*[2] The broad range of zeolite applications is a consequence of their specific chemical compositions and unique porous structures. Therefore, the search for new zeolites has become a continuous interest in the field of zeolite science since the pioneering work reported by Barrer in the 1940s.[3] In general, zeolite materials are synthesized under hydrothermal–solvothermal conditions, and the reaction gel medium contains the framework atoms, solvents, templates or structure-directing agents (SDAs), and mineralizers. Systematization and understanding of zeolite synthesis have been tremendous, but the detailed molecular mechanism of zeolite nucleation is still unknown.[4] This makes it difficult to realize the "*ab initio*" synthesis of a desired new structure.[5,6]

Nevertheless, in the last decade, several new synthetic strategies have been developed towards the synthesis of zeolites with specific structures and properties based on the utilization of pre-designed organic structure-directing agents,[7] heteroatom substitution,[8] topotactic transformations,[9,10] and charge density mismatch,[11] *etc.* On the other hand, the advancement of structure determination and computer simulation techniques has greatly enhanced the researchers' ability to obtain structure solutions of complex zeolite structures, as well as the prediction of hypothetical zeolite structures. The progress in synthesis and structure determination has led to the rapid developments in discovering new zeolite framework structures.[12] Up to 2007 (the sixth edition of Atlas of Zeolite Framework Types), 176 distinct zeolite framework types have been approved by Commission of the International Zeolite Association (IZA-SC). To date, the number of IZA structures has increased to 225,[13] while some new zeolite frameworks have not been approved by IZA-SC yet. Compared to the previously known zeolite framework types, some interesting structural features are found in these newly discovered zeolites, such as hierarchical pores, odd-ring numbers (11-, 15-rings), extra-large pores (16-, 18-, 20-, 28-, and 30-rings),

[a] *State Key Laboratory of Inorganic Synthesis and Preparative Chemistry, College of Chemistry, Jilin University, Changchun 130012, P. R. China. E-mail: jihong@jlu.edu.cn*

[b] *Instituto de Tecnología Química (UPV-CSIC), Universidad Politécnica de Valencia, Consejo Superior de Investigaciones Científicas, 46022, Valencia, Spain*

Jiyang Li obtained her PhD degree from Jilin University in 2000, and worked as Humboldt Research Fellow at Göttingen University (Germany, 2001–2003). Since 2008, she has been a full Professor in the State Key Laboratory of Inorganic Synthesis and Preparative Chemistry, Jilin University. Her research interest is focused on the synthesis and properties of novel zeolitic materials.

Avelino Corma received his PhD degree from the Universidad Complutense de Madrid in 1976. He carried out postdoctoral research in the Department of chemical engineering at Queen's University (Canada, 1977–1979), and since 1990 he has been a research professor at the Instituto de Tecnología Química (UPV-CSIC) at the Universidad Politécnica de Valencia. His research focuses on acid–base and redox catalysis, and zeolite synthesis.

chiral pores, and extremely complex framework topologies. The findings of these new zeolites not only enrich the structural chemistry of zeolites, but can also enlarge the potential applications of zeolites in catalysis and sorption–separation.

In this review, we will focus on the synthesis of new zeolites during the last decade. Three synthetic strategies that have led to the discovery of new zeolites with novel structural features will be described: (a) using pre-designed organic SDAs including quaternary and diquaternary SDAs, P-containing SDAs, proton sponges, imidazolium derivatives, and metal complexes; (b) using heteroatom substitutions in aluminophosphates, silicates, and germanates; (c) using topotactic transformations of 2D–3D, 3D–2D–3D, and 3D–3D structures. Finally, we will present the challenges and perspectives facing the synthesis of new zeolites in the future.

2. Zeolites synthesized by using pre-designed organic structure-directing agents

The synthesis of zeolites usually involves the use of alkali metal ions or organic amines/ammonium cations as templates or SDAs. Particularly, the synthesis of high-silica, aluminophosphate, and germanosilicate zeolites presents more dependence on the use of organic SDAs. A wide range of organic species can be used as SDAs, and these organic SDAs have been recognized as some of the most important factors to determine the zeolite formation. Studies show that the pore openings, pore dimensions and their connectivities, and pore architectures of the synthesized zeolites can be modified by varying the shape, size, charge, rigidity, polarity, and hydrophobicity of organic SDAs. Thus, the rational design of organic SDAs is one of the most efficient approaches for the synthesis of novel zeolite structures.[7,14] In this section, we will present some successful examples achieved in the last few years by using pre-designed organic SDAs including quaternary and diquaternary SDAs, P-containing SDAs, proton sponges, imidazolium derivatives, and metal complexes.

2.1 Quaternary SDAs

The organic quaternary ammonium cations are commonly used SDAs for the preparation of high-silica zeolites. In the past few years, some novel quaternary SDAs have been designed with the aim of controlling the pore dimensions and synthesizing new zeolites. In 2003, Elomari *et al.* developed a synthetic strategy based on enamine chemistry for the synthesis of novel quaternary SDAs.[15] More specifically, cyclic ketones are reacted with cyclic amines, and then reduced, finally a fourth group is added to the nitrogen to produce charged quaternary SDAs. This procedure allows the synthesis of series of bulky and rigid organic SDAs, resulting in the discovery of new high-silica zeolites. A notable example is the high-silica zeolite SSZ-57 (***SFV**) synthesized by using SDA **1** in hydroxide media.[16] SSZ-57 is the most complex structure known so far, which contains 99 crystallographically distinct T atoms. Its structure has been determined by applying the advanced crystallographic techniques to high quality single-crystal X-ray diffraction data collected for a microcrystal.[17] The idealized structure of SSZ-57 is related to that of ZSM-11 (**MEL**) that can be synthesized with the same SDA of SSZ-57 in the fluoride media. One of the 16 10-ring channels in ZSM-11 is replaced by a 12-ring channel in the structure of SSZ-57, generating the three-dimensional (3D) channel system composed of intersecting 12-ring, 10-ring, and 10-ring channels along the [100], [010], and [100] directions.

Interestingly, slight changes in SDA **1** lead to different zeolite structures, indicating the high selectivity between the SDAs and zeolite structures obtained (see Table 1).[18] Starting from SDA **1**, changing the butyl group by methyl/ethyl groups yields aluminosilicate ZSM-12 (**MTW**) with 1D 12-ring channels. Meanwhile, the use of a cyclo-octyl ring instead of a cyclo-hexyl ring in **1** produces another new borosilicate zeolite SSZ-58 (**SFG**) with 2D 10-ring channels and large cavities. Further attaching a methyl group to the pyrrolidine ring produces aluminosilicate ZSM-11 (**MEL**) with 3D 10-ring channels.

In the case of extra-large pore zeolites, a novel germanoaluminosilicate zeolite ITQ-43 has been prepared with a hierarchical

Table 1 SDAs related to *N*-butyl-*N*-cyclohexyl-pyrrolidinium (**1**) and their resulting zeolite structures

SDA	Zeolitic product	Framework composition	Channel system
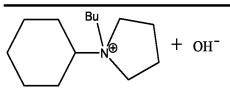 **1**	SSZ-57 (***SFV**)	Si	3D, 12R × 10R × 10R
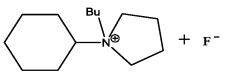 **1**	ZSM-11 (**MEL**)	Si, Al	3D, 10R × 10R × 10R
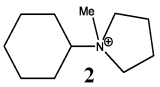 **2**	ZSM-12 (**MTW**)	Si, Al	1D, 12R
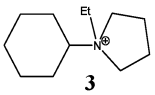 **3**	ZSM-12 (**MTW**)	Si, Al	1D, 12R
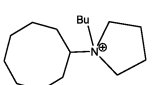 **4**	SSZ-58 (**SFG**)	Si, B	2D, 10R × 10R
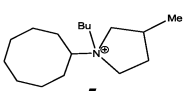 **5**	ZSM-11 (**MEL**)	Si, Al	3D, 10R × 10R × 10R

Jihong Yu received her PhD degree from Jilin University in 1995, and worked as a postdoctoral fellow first at the Hong Kong University of Science and Technology and then at Tohoku University (Japan) from 1996–1998. She has been a full Professor in the Chemistry Department, Jilin University, since 1999. She was awarded the Cheung Kong Professorship in 2007. Her main research interest is in the rational design and synthesis of nanoporous materials.

mesoporous-microporous structure by using SDA **6**.[19] The framework of ITQ-43 has 1D cloverleaf-like 28-ring channels (21.0 Å × 19.6 Å) running along the [001] direction, which are further connected by 2D 12-ring channels along the [100] direction (6.8 Å × 6.1 Å) and the ⟨110⟩ direction (7.8 Å × 5.7 Å). Later, seven isoindoline-based organic SDAs with increasing sizes have been designed by Yu and coworkers to systematically study the synthesis of extra-large pore zeolites.[20] As a result, eight germanosilicate zeolites have been produced (Fig. 1). Studies show that the relatively small SDAs or large and very flexible SDAs yield Beta (***BEA**), ITQ-7 (**ISV**), or ITQ-17 (**BEC**). Upon increasing the size of organic SDAs above a certain dimension, extra-large pore zeolites including ITQ-15 (**UTL**), ITQ-37 (-**ITV**), ITQ-44 (**IRR**), and ITQ-43 have been obtained.

Novel rigid polycyclic SDAs can be generated by using Michael addition reaction. Using this method, a unique polycyclic quaternary SDA **7** has been prepared, which gives rise to a new aluminosilicate zeolite SSZ-52 (**SFW**) under high OH^-/Si conditions and in the presence of Al (Fig. 2).[21] SSZ-52 is a member of the ABC-6 zeolite family, and its structure features an 18-layer stacking of hexagonally arranged 6-rings. The large cavities containing two bulky organic SDAs are found in such a structure, which are connected to generate 3D 8-ring channels. Also using bulky polycyclic SDA **8**, a new high-silica zeolite SSZ-61 (*-**SSO**) has been produced under relatively dilute conditions using F^- ions as the mineralizer (Fig. 2).[22] SSZ-61 possesses dumbbell-shaped extra-large 18-ring channels. Its framework is closely related to those of ZSM-12 (**MTW**) and SSZ-59 (**SFN**), in which the same layers are found, but their connection modes are different.

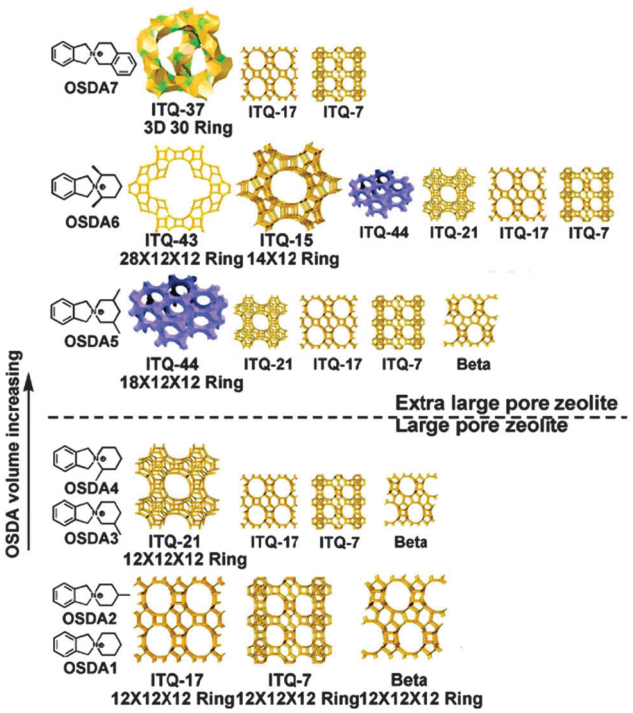

Fig. 1 Relationship between the different sizes of SDAs and the resulting products in high-throughput synthesis of germanosilicate zeolites. Reprinted with permission from ref. 20. Copyright 2008 American Chemical Society.

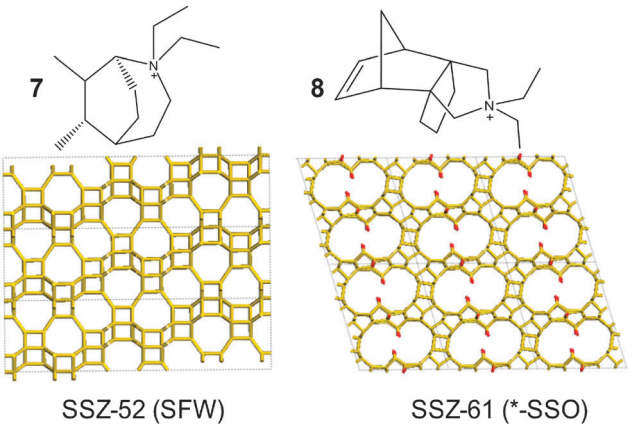

Fig. 2 Polycyclic quaternary SDAs used in the syntheses of SSZ-52 and SSZ-61.

Burton and coworkers have designed more flexible quaternary ammoniums that have one or more (unfused) ring structures for the discovery of new zeolites.[23] The reduction of amides (or lactams), enamines, or nitriles is used to prepare the precursor amines. By using this kind of SDA, several zeolites including SSZ-53 (**SFH**), SSZ-55 (**ATS**), SSZ-57 (***SFV**), SSZ-58 (**SFG**), SSZ-59 (**SFN**), SSZ-60 (**SSY**), SSZ-63, SSZ-64, and a new zeolite SSZ-65 (**SSF**) have been synthesized.

2.2 Diquaternary SDAs

The diquaternary ammonium cations composed of rigid rings and flexible methylene chains are a class of feasible SDAs, which have led to the synthesis of a variety of novel zeolites. For example, the high-silica zeolites SSZ-74 (-**SVR**), IM-5 (**IMF**) and TNU-9 (**TUN**) have been synthesized by using diquaternary SDAs built from *N*-methyl pyrrolidine heterocycles and the methylene chains with different lengths (Fig. 3). The structures of these zeolites are reminiscent of that of **MFI**, all of them possess multi-dimensional 10-ring channels. However, their syntheses are sensitive to the size difference of diquaternary

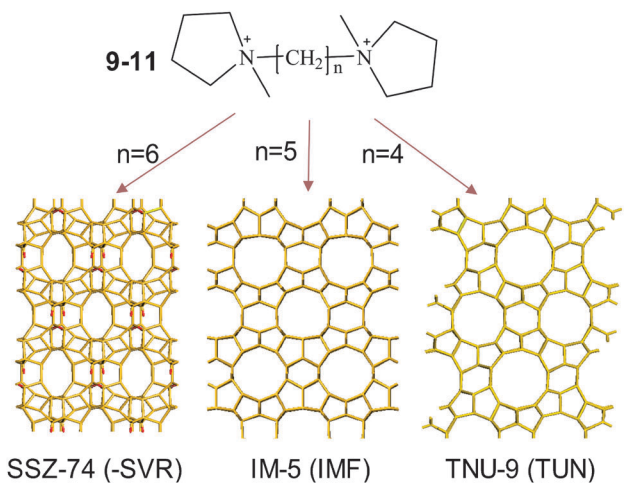

Fig. 3 Varying chain length of diquaternary SDAs leads to different high-silica zeolites.

SDAs used. SSZ-74 is obtained in the fluoride media with SDA **9**,[24] which has 3D intersecting 10-ring channels running along the [110], [010], and [001] directions. IM-5 is prepared by using SDA **10**,[25] which features 2D 10-ring channels parallel to *a* and *c*, respectively. Whereas TNU-9 is synthesized in the presence of SDA **11** and Na^+ ions as SDAs,[26] whose 3D pore system consists of two parallel 10-ring channels along the [010] direction connected by 10-ring openings along the [10$\bar{1}$] direction. Notice that all of these three zeolites have complex structures containing 24 crystallographically distinct T sites, which are solved by the combination of powder diffraction and electron microscopy techniques.

Zones and coworkers designed five different types of diquaternary SDAs by varying the heterocycles, and keeping constant the methylene chain lengths of C4, C5, and C6. They systemically study the synthesis in the silica system involving the diquaternary SDAs, $TMA^+/Na^+/OH^-/F^-$ ions, and B/Ge/Al heteroatoms.[27] As listed in Table 2, 18 different zeolite topologies have been produced by using 15 diquaternary SDAs, and their pore openings vary from small pores (6- and 8-rings), to medium pores (10-rings), and to large pores (12-rings). The size and shape of heterocycles and the $-CH_2-$ chain lengths have an influence on the resulting zeolite structures. Moreover, the additional inorganic species, such as $TMA^+/Na^+/OH^-/F^-$ and B/Ge, also control the products formed.

Recently, a new diquaternary SDA **12** with more heterocycles has been synthesized by the reaction of a dihalidealkane (such as 1,6-dibromobutane) with *N*-cyclohexylpyrrolidine. This SDA has led to the discovery of SSZ-82 (**SEW**) zeolite with a 2D pore system of 10-ring and 12-ring channels.[28]

Diquaternary SDAs without heterocycles, such as SDA **13–15** with different lengths of the methylene chain, can direct the synthesis of zeolites ITQ-13 (**ITH**), ITQ-24 (**IWR**), and silicate octadecasil (**AST**). By using SDA **16**, a new germanosilicate zeolite IM-17 (**UOV**) has been produced in both of OH^- and F^- media.[29] Its framework possesses a 3D pore system made of intersecting 8-, 10-, and 12-ring channels running along the [100], [001], and [100] directions, respectively. With SDA **17**, a new aluminophosphate zeolite EMM-3 (**EZT**) containing 1D 12-ring channels has been synthesized.[30]

In the above cases, the size of the diquaternary SDAs, determined by the length of the methylene chain and the shape of head groups, obviously affect the size and connection modes of the resultant channels or cages, resulting in the formation of different zeolite topologies. Meanwhile, the size of organic SDAs also influences the amount of negative charges in the framework, thus affecting the framework compositions. This is important for the synthesis of zeolites with high thermal stability (high silica) and strong Brönsted acidity. In addition, the linear diquaternary SDAs have more flexibility. A higher flexibility of the SDA can result in a lower selectivity for a particular structure but opens up the possibility of synthesizing different structures. Indeed, the configuration of the organic SDAs can be altered according to the different surroundings of inorganic species, which favours the formation of new zeolite structures.

In principle, more open structures can be achieved by increasing the size of the organic SDAs. Thus, by using the large SDA **18** with four chiral centers, a chiral germanosilicate zeolite ITQ-37 (**-ITV**) with single gyroidal channels has been synthesized (Fig. 4).[31] ITQ-37 possesses extra-large 30-ring channels, which is the largest in the known zeolites to date. Such an open channel system leads to its low framework density of 10.3 T/1000 $Å^3$. The unique cavities comprising the enantiomorphous *srs* nets are found in the framework. The framework and channel systems have the opposite chirality: the framework with left-handedness and the channel system with right-handedness. Notice that another organic SDA **19** can also be used for the synthesis of chiral ITQ-37.[32]

In addition, a new type of unsymmetrical diquaternary cations has been prepared for the synthesis of zeolites with interconnected medium and large pores. As shown in Fig. 5, the SDA **20** is designed by combination of the rigidity and the flexibility of SDAs used in the syntheses of large-pore (*i.e.*, ZSM-12) and medium-pore (*i.e.*, ZSM-5) zeolites, respectively. Employing the designed SDA **20**, a new aluminosilicate zeolite ITQ-39 (***-ITN**)

Table 2 Five different types of diquaternary SDAs and the resulting zeolite structures

Diquaternary SDA	Framework type	Pore system
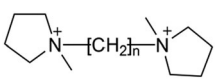	***BEA**	3D, 12R × 12R × 12R
	BEC	3D, 12R × 12R × 12R
	IWW	3D, 12R × 10R × 8R
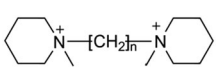	**MTW**	1D, 12R
	MOR	1D, 12R
	***STO**	1D, 12R
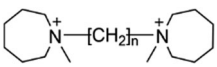	**SSY**	1D, 12R
	TUN	3D, 10R × 10R × 10R
	IMF	3D, 10R × 10R × 10R
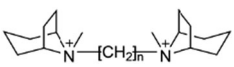	**-SVR**	3D, 10R × 10R × 10R
	MFI	3D, 10R × 10R × 10R
	STI	2D, 10R × 8R
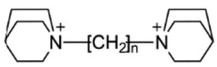	**STF**	1D, 10R
	AFX	3D, 8R × 8R × 8R
	RUT	0D, 6R
(n = 4, 5, 6)	**AST**	0D, 6R
	NON	0D, 6R
	DOH	0D, 6R

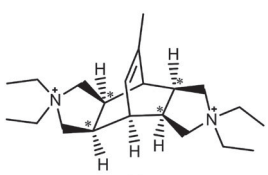

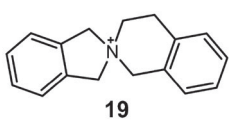

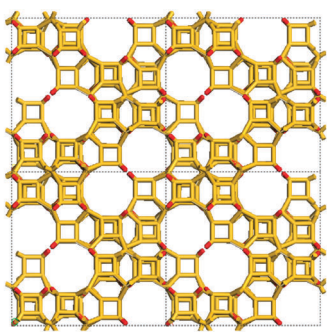

Fig. 4 Two SDAs used in the synthesis of ITQ-37.

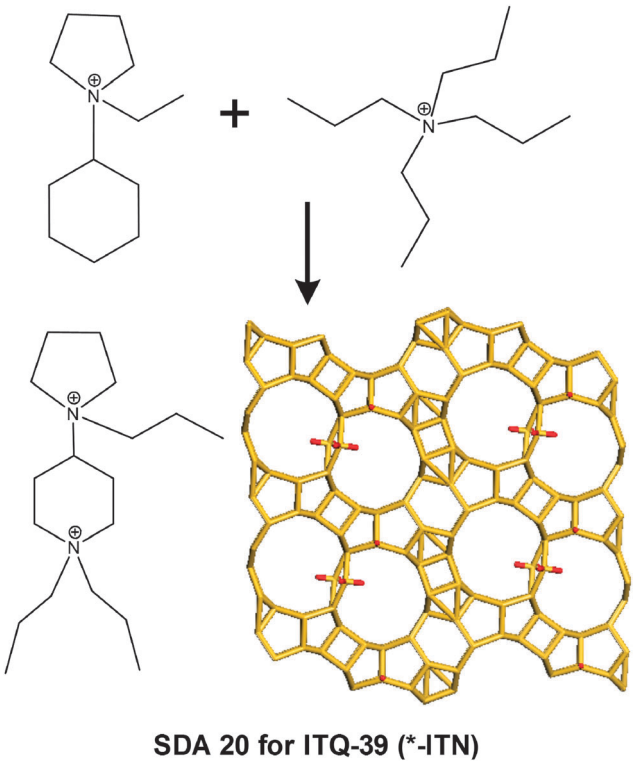

Fig. 5 Organic SDA designed for the synthesis of ITQ-39 by combination of the rigidity and flexibility of SDAs used in the synthesis of ZSM-12 and ZSM-5, respectively.

has been discovered.[33] ITQ-39 exhibits similar disorder to that of zeolite Beta. Its framework possesses a possible 3D large pore (12-ring) system with available pore opening between those of Beta and ZSM-5, or a 3D pore system with large (12-ring) and medium (10-ring) intersecting pores.[34] As with ITQ-39, a new multipore zeolite ITQ-38 (**ITG**) with large and medium pores has been prepared by using a similar diquaternary SDA.[35]

2.3 Phosphorus-containing organic SDAs

Besides the traditionally used amine and ammonium SDAs, a new type of phosphorus-containing SDAs has been explored to synthesize new zeolite structures with large-pore and multi-dimensional channels. The phosphorus-containing SDAs are typically known as phosphonium, phosphazenes, and amino-phosphine cations. These SDAs are more thermally stable than the amine/ammonium SDAs and allow more severe crystallization conditions since the Hoffman degradation does not occur in the synthesis.

As shown in Fig. 6, the validity of using phosphonium cations as SDAs has been demonstrated in the syntheses of new zeolites ITQ-26 (**IWS**),[36] ITQ-27 (**IWV**),[37] and ITQ-34 (**ITR**).[38] In the synthesis, F^- ions are used as a mineralizer and induce the formation of small cages (such as *d*4*r*). Germanosilicate ITQ-26 (**IWS**) with a 3D 12-ring large-pore system is synthesized by using SDA **21**.[36] SDA **22** is used to synthesize aluminosilicate ITQ-27 (**IWV**) with 2D intersecting 12-ring and 14-ring channels.[37] Such an SDA is prepared by methylation of diphenylphosphine with methyl iodide in chloroform in the presence of K_2CO_3, then it is changed to the hydroxide salt with an anionic exchange resin. Notably, the synthesis of ITQ-27 needs relatively long crystallization times (59 days).

The prominent directing role of phosphonium SDAs is more obvious in the synthesis of zeolite ITQ-34 (**ITR**). ITQ-34 with connected 9-ring and 10-ring channels has been first discovered as the polymorph B of the zeolite ITQ-13 (**ITH**, polymorph A).[38] ITQ-13 can be synthesized by using SDA **23**.[39] An attempt to prepare ITQ-34 with the same SDA only leads to the mixture of ITQ-13 and ITQ-34. Several similar SDAs with shorter dicationic

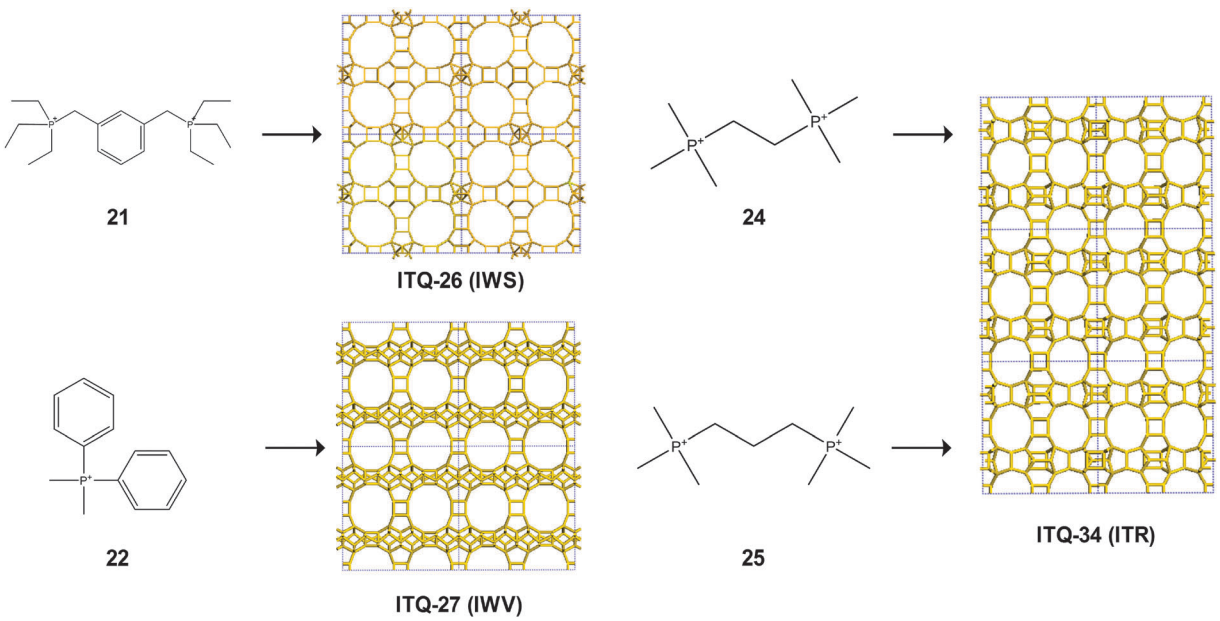

Fig. 6 Phosphonium cations as SDAs used in the syntheses of ITQ-26, ITQ-27, and ITQ-34.

chains such as ethane-1,2-, propane-1,3-, and butane-1,4-bis-(trimethylammonium) do not favour the synthesis of either ITQ-13 or ITQ-34, however, their corresponding bis(trimethylphosphonium) cations **24** and **25** can yield pure ITQ-34. The structure-directing role of P-containing SDAs in the formation of ITQ-34 has been elucidated by theoretical calculations of the short-range and long-range van der Waals interactions between zeolite and SDAs.

On the other hand, by using SDA **26** (Fig. 7), a new germanosilicate zeolite ITQ-49 (**IRN**) with unusual odd 7-ring units has been prepared in the presence of Ge and F^- species.[40] It is a small-pore zeolite containing 8-ring channels and large non-spherical cavities.

Significantly, a new type of SDA based on phosphazenes has been investigated for the synthesis of zeolites. These SDAs exhibit several advantages: (1) easy construction by the building-block units in a similar way to "Lego chemistry"; (2) a large number of alkyl groups; (3) adequate polarity and stability; (4) mobilization of silica or other heteroatoms in the reaction gel through their high basicities; (5) nearly unlimited synthesis flexibility. Such SDAs may provide more opportunity to direct the formation of particular zeolite structures than quaternary ammonium or phosphonium SDAs. With this type of SDA **28**, ITQ-47 with the **BOG** topology is obtained (Fig. 8). Its framework has Si–B–O composition instead of Si–Al–O occurring in boggsite that is a rare natural zeolite difficult to be synthesized.

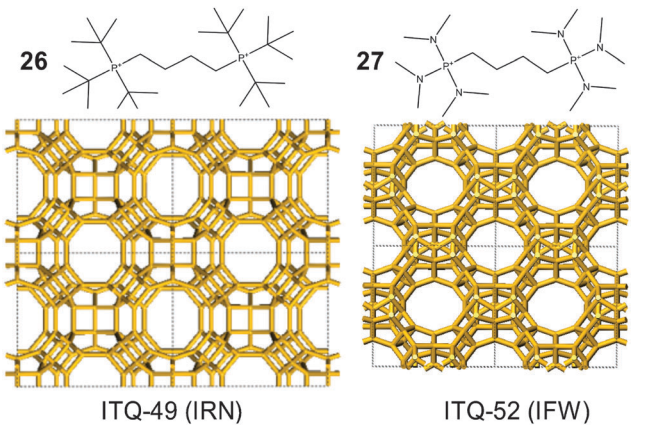

Fig. 7 P-containing SDAs used in the syntheses of ITQ-49 and ITQ-52.

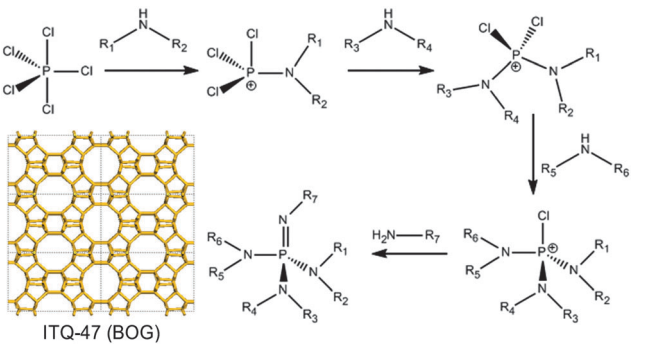

Fig. 8 Phosphazene SDAs prepared by "Lego chemistry" and the structure of ITQ-47.

In addition, the aminophosphines containing P–C and P–N bonds that are related to phosphoniums and phosphazenes are also found to facilitate the synthesis of novel zeolites, such as zeolite **STF**, ITQ-52, and other unidentified solids. By using SDA **27**, a silicoborate zeolite ITQ-52 (**IFW**) has been prepared with a particularly interesting structure that combines medium (10-ring) and small (8-ring) pores (Fig. 7).[41]

2.4 Proton sponges as SDAs

Bulky aromatic proton sponges as newly developed organic SDAs show their advantage in directing extra-large pore zeolites due to their high basicity along with the large size and rigidity. Their high basicity makes their protonation in the synthetic media, enhancing the inorganic–organic interactions during the nucleation. The large size and rigidity of organic SDAs may offer "proton sponges" with a suitable molecular structure for templating extra-large pores. A new extra-large pore silicoaluminophosphate zeolite ITQ-51 (**IFO**) has been synthesized with the commercially available SDA **29** (Fig. 9).[42] ITQ-51 is the first aluminophosphate-based zeolite possessing 16-ring channels. Importantly, ITQ-51 is stable upon calcination at 550 °C after the removal of organic SDAs, being a rare example of hydrothermally stable extra-large pore zeolites. A variety of proton sponge SDAs designed with different sizes, geometries, hydrophobicity, or basicity may lead to the discovery of more new zeolite structures.

2.5 Imidazolium derivatives as SDAs

Imidazolium derivatives as SDAs also promote the discovery of new zeolite structures. Early work is the zeolites **TON**, **MTT**, **MTW**, and **ITW** synthesized by using imidazolium-based SDAs in basic media or in fluoride media.[43,44] Recently, the use of SDAs **30** and **31** results in the synthesis of germanosilicate zeolites IM-16 (**UOS**)[45] and IM-20 (**UWY**)[46] (Fig. 10), respectively. The structure of IM-16 possesses 10-ring channels along the [100] direction and intersecting 8-ring channels along the [010] and [001] directions. The 3D channel system of IM-20 is formed by the intersecting 12-ring channels parallel to the *c*-axis and 10-ring channels parallel to *a*-, *b*- and *c*-axis.

Silicogermanate zeolite SU-32 (**STW**) is one of the rare chiral zeolites. Its framework contains helical 10-ring channels running along the [010] direction and intersected 8-ring channels running along the [100], [010], and [110] directions. It was first

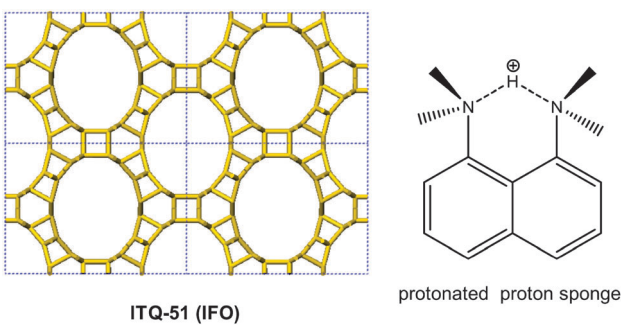

Fig. 9 Structure of ITQ-51 zeolite and SDA **29** used in the synthesis.

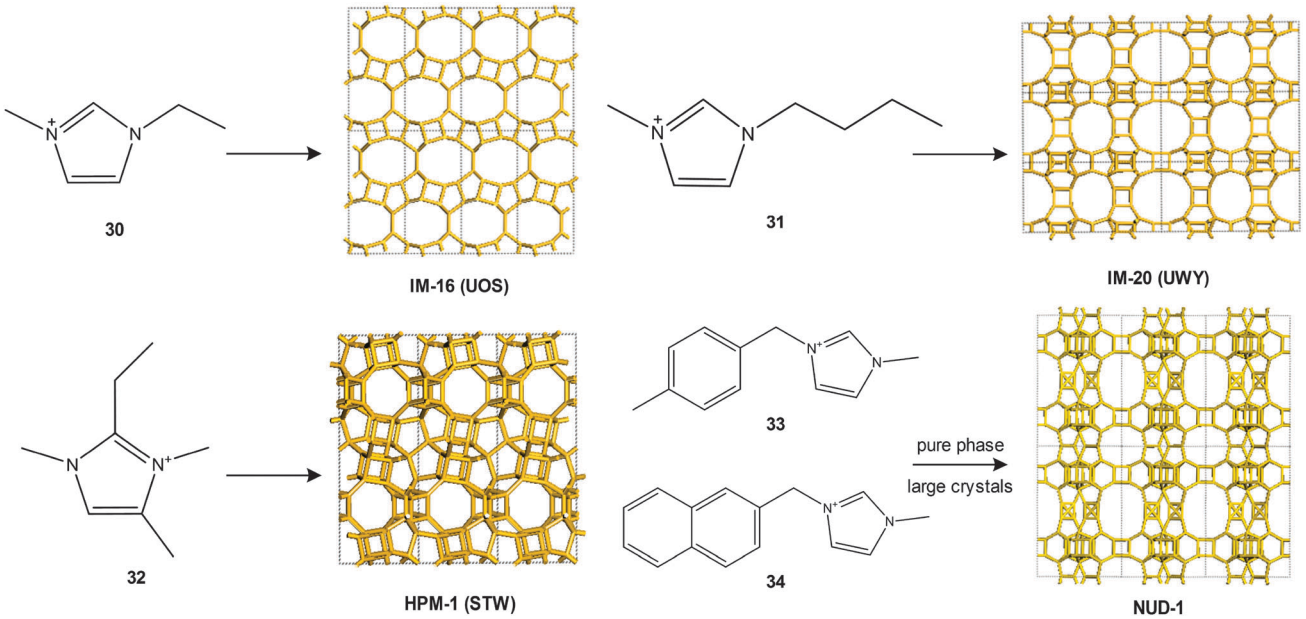

Fig. 10 Imidazolium-based SDAs used in the syntheses of IM-16, IM-20, HPM-1, and pure phase and large crystals of NUD-1.

synthesized by using diisopropylamine as an SDA,[47] but its low stability due to the high Ge content (Ge/Si >1) in the framework limits its application. By using imidazolium derivative **32** as an SDA, the first pure silica chiral zeolite HPM-1 with **STW** topology has been successfully prepared (Fig. 10).[48]

Supramolecular self-assembly of aromatic SDAs has proven to be an effective approach to direct the formation of zeolites.[49] This has been demonstrated in the synthesis of ITQ-29 (**LTA**) and $AlPO_4$-5 (**AFI**). More recently, this concept is first applied in the synthesis of a new extra-large pore germanosilicate zeolite NUD-1 by using imidazolium-based SDAs.[50] The pure phase of NUD-1 is synthesized by using SDA **33**, while the large crystals of NUD-1 are obtained with SDA **34** (Fig. 10). The extra-large 18-ring channels of NUD-1 are running along the *c* axis, which are intersected with the 10-ring and 12-ring channels running along the *a* and the *b* axis, respectively. Although the locations of SDAs are not determined due to the disorders, the self-assembled aggregates of SDAs in the structure of NUD-1 are confirmed by photoluminescent studies of the SDAs in diluted and concentrated solution, as well as in zeolite NUD-1.

2.6 Metal complexes as SDAs

Metal complexes can be used as SDAs to direct the extra-large pore or chiral zeolite structures because of their special and rigid conformation. A successful example in the previous work is UTD-1 (**DON**), the first high-silica extra-large pore zeolite with 1D 14-ring channels synthesized by using SDA **35** or **36**.[51] Recently, Yu and coworkers reported a new gallogermanate zeolite GaGeO-CJ63 (**JST**) structurally directed by the *in situ* formed chiral metal complex **37** in the reaction system (Fig. 11).[52] GaGeO-CJ63 possesses 3D intersecting 10-ring channels running along the [100], [010], and [001] directions. Its structure is constructed exclusively by 3-rings, resulting in the low framework density of 10.5 T/1000 Å^3. Two unique

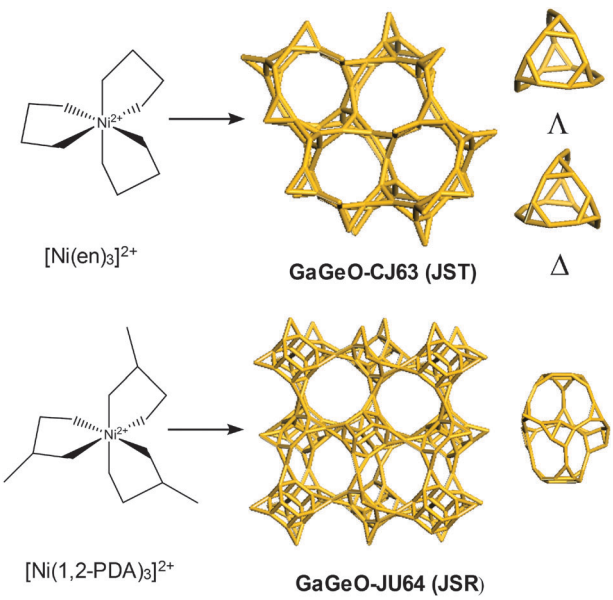

Fig. 11 Metal complexes used as SDAs in the syntheses of GaGeO-CJ63 with chiral [$3^4{\cdot}6{\cdot}10^3$] cavities and GaGeO-JU64 with chiral [$3^{12}{\cdot}4^3{\cdot}6^2{\cdot}11^6$] cavities.

cavities are found in its framework, and the racemic $[Ni(en)_3]^{2+}$ cations are located in the chiral [$3^4{\cdot}6{\cdot}10^3$] cavities with the same handedness, indicating the chirality transfer from the chiral SDA to inorganic framework.

Later, by using the *in situ* synthesized chiral SDA **38**, another novel gallogermanate zeolite GaGeO-JU64 (**JSR**) has been synthesized (Fig. 11).[53] Its structure contains unprecedented 3D intersecting odd 11-ring channels running along three orthogonal directions (Fig. 11). GaGeO-JU64 has the lowest framework density of 9.9 T/1000 Å^3 among the known oxide zeolites to date. The racemic $[Ni(1,2\text{-}PDA)_3]^{2+}$ cations induce

pairs of chiral [$3^{12}\cdot4^3\cdot6^2\cdot11^6$] cavities in the framework of GaGeO-JU64.

Recently, a series of zeolites with small 8-ring pores, such as Cu-SAPO-34, Cu-SSZ-13, and Cu-SAPO-18, which are important catalysts for the selective reduction (SCR) of NO_x, have been prepared by using Cu amino complexes,[54–58] either as the only SDAs or in combination with the conventional SDAs. This procedure has the advantage of avoiding one step, *i.e.*, the cation exchange with Cu, during catalyst preparation. The resultant materials are shown to be highly active and hydrothermally stable.

Above we have demonstrated that the utilization of novel pre-designed SDAs allows the synthesis of many new zeolites. The resulting novel zeolites exhibit unprecedented structural features, such as hierarchical pores, odd ring numbers, extra-large pores, chiral pores, and extremely complex framework topology. These unique structures may offer new perspectives for zeolite materials in catalysis and adsorption–separation. The designed SDAs typically possess complex structures of rigid rings and flexible chains, and most of them are prepared by complex reaction schemes including Diels–Alder, Mannich, Michael addition reactions, which are not commercially available. However, we cannot exclude the opportunity to obtain new zeolites by using commercially available and simple SDAs as in the cases of the syntheses of zeolites STA-15 (**SAF**, tetrapropylammonium hydroxide), and UZM-5 (**UFI**, mixture of tetramethylammonium and tetraethylammonium). Since a large number of hypothetical zeolite structures have been designed and can be predicted to be chemically feasible according to the local interatomic distance (LID) criteria,[59] in the future, more efforts should be devoted to the design of novel SDAs by systematic modification of the large variety of organic species, particular to the "*ab initio*" design of the organic SDAs towards the synthesis of target hypothetical zeolites. Notice the fact that an SDA might stabilize more than one microporous framework, other synthetic factors, such as crystallization temperature and time, pH, gel concentration and ratios, also influence the zeolite formation. The templating role of SDAs becomes operative only in the gel with right gel chemistry.

3. Zeolites synthesized by using heteroatom substitution

Zeolites are strictly defined as those built up from TO_4 tetrahedra (T = Si, Al, P). Other elements, such as B, Be, Mg, Ga, Ge, Zn, and Co, can isomorphically substitute the zeolite framework. The introduction of some heteroatoms (except Si, Al, P) in the zeolite framework may generate special chemical and physical properties, such as catalysis, magnesium, and luminescence, *etc.* Moreover, heteroatoms have a great influence on the formation of zeolites. For example, heteroatoms Ge, B, Ga, Zn, and Be favour the formation of some particular building units (*e.g.*, 4-rings, 3-rings, *d*4*r*, *d*3*r*, spiro-5 units, *etc.*) due to their suitable T–O bond and T–O–T angles that can stabilize these building units. The initial work of heteroatom substitution is focused on the synthesis of the analogues of known aluminophosphate or aluminosilicate zeolites but with different properties. In the past few years, by introducing heteroatoms in the synthesis, many novel zeolites with low-framework density, extra-large pores, and chiral pores have been synthesized. In this section, we mainly describe the new zeolites obtained by heteroatom substitution of T sites in aluminophosphates, silicates and germanates, as well as of O sites in zeolites.

3.1 Heteroatom substitution in aluminophosphates (AlPOs)

The structure of aluminophosphate (AlPO) zeolites is constructed by the strict alternation of AlO_4 and PO_4 tetrahedra. The Al and P atoms in the framework can be easily substituted by heteroatoms to form MAPO molecular sieves (M = heteroatom). Various elements with different valences can be incorporated into the MAPO zeolites, such as +1 (Li), +2 (Be, Mg, Ca, Zn, Mn, Fe, Co, Ni, Cu, Cd, Sr), +3 (Cr, Co, Fe, Ga, Mo), +4 (Ge, Ti, Sn, Zr, V), and +5 (As, V, Nb).[8] The isomorphous substitution of heteroatoms for Al/P sites in the framework may generate known AlPO zeolite analogues. Importantly, in some cases, the heteroatoms may stabilize the framework and induce novel zeolite structures. So far, nearly 30 MAPO zeolites with new topologies have been synthesized (Table 3). All of these new MAPO zeolites cannot be produced in a similar pure AlPO synthetic system, which highlights the important role of heteroatoms in the synthesis.

By introducing the divalent metal as a heteroatom, the first heteroatom-containing chiral AlPO zeolite MAPO-CJ40 (M = Co, Zn) with **JRY** zeotype has been synthesized by Yu and coworkers.[60] MAPO-CJ40 crystallizes in the chiral $P2_12_12_1$ space group. Its framework possesses 1D helical 10-ring channels, which are made of double-helical ribbons with the same handedness (Fig. 12). Of the three distinct Al sites in the framework, the heteroatoms occupy the Al (1) position, forming a helical array along the 10-ring channels. The theoretical study indicates that the Al (1)-centered tetrahedron has high geometric distortion far from the ideal one. The incorporation of heteroatoms may relax the high distortion, thus stabilizing the whole chiral framework.

Also choosing Co and Zn as heteroatoms, two new zeolites MAPO-CJ62 (**JSW**) and MAPO-CJ69 (**JSN**) (M = Co, Zn) with 8-ring channels have been synthesized by using SDA **39** and **40**, respectively.[61,62] In MAPO-CJ62, the heteroatoms are orderly distributed, and selectively occupy two of the three distinct metal crystallographically positions in the framework, while in MAPO-CJ69, the heteroatoms occupy the same position with Al atoms in the framework.

In the presence of Zn as a heteroatom, two new zeolites ZnAPO-57 (**AFV**) and ZnAPO-59 (**AVL**) have been synthesized by using SDA **41** and **42**, respectively.[63] ZnAPO-57 and ZnAPO-59 represent new members of the ABC-6 family, and both of them possess a 2D 8-ring pore system. In the synthesis, the addition of different heteroatoms including Zn, Mg, and Si, *etc.*, and changing the SDA/H_3PO_4 ratios may vary the framework charge density and yield different zeolite structures. At a high SDA/H_3PO_4 ratio, the introduction of Si in the synthesis of MAPO-57 or MAPO-59 produces **BPH** zeolite, while decreasing the SDA/H_3PO_4 ratio results in **LEV** zeolite.

Table 3 Structures and compositions of new MAPO zeolites without AlPO analogues[a]

Type material	Framework type code	Heteroatom	Channel system
ACP-1	**ACO**	Co, Fe	3D, 8R × 8R × 8R
MAPO-46	**AFS**	Co, Mg, Mn, Ni, Zn, Si	3D, 12R × 8R × 8R
ZnAlPO-57	**AFV**	Zn, Mg, Si, Zn, Si	2D, 8R × 8R
SAPO-56	**AFX**	Mg, Co, Mn, Si, Zr	3D, 8R × 8R × 8R
CoAPO-50	**AFY**	Co, Zn, Mg, Mn	3D, 12R × 8R × 8R
ZnAlPO-59	**AVL**	Zn, Mg, Si, Zn	2D, 8R × 8R
Beryllophosphate-H	**BPH**	Mg, Zn, Si	3D, 12R × 8R × 8R
DAF-1	**DFO**	Co, Mg, Ni	3D, 12R × 10R × 8R
DAF-2	**DFT**	Co	3D, 8R × 8R × 8R
Edingtonite	**EDI**	Co, Cu	3D, 8R × 8R × 8R
Faujasite	**FAU**	Co, Cu, Zn, Si	3D, 12R × 12R × 12R
CoAPO-CJ40	**JRY**	Co, Zn, Mn, Fe	1D, 10R
CoAPO-CJ69	**JSN**	Co, Zn	2D, 8R × 8R
CoAPO-CJ62	**JSW**	Co, Zn	1D, 8R
Laumontite	**LAU**	Co, Zn, Mn, Fe,	1D, 10R
Merlinoite	**MER**	Co	3D, 8R × 8R × 8R
UiO-28	**OWE**	Co, Mg	2D, 8R × 8R
Phillipsite	**PHI**	Co, Zn	3D, 8R × 8R × 8R
Rho	**RHO**	Co, Mn, Mg	3D, 8R × 8R × 8R
STA-1	**SAO**	Zn, Mg	3D, 12R × 12R × 12R
STA-6	**SAS**	Mg, Mn, Fe, Zn, Co	1D, 8R
STA-2	**SAT**	Mg	3D, 8R × 8R × 8R
Mg-STA-7	**SAV**	Co, Zn, Mg, Mn, Fe	3D, 8R × 8R × 8R
UCSB-8Co	**SBE**	Co, Zn, Mg, Mn	2D, 12R × 8R
UCSB-6GaCo	**SBS**	Co, Zn, Mg, Mn	3D, 12R × 12R × 12R
USCB-10GaZn	**SBT**	Co, Zn, Mg	3D, 12R × 12R × 12R
SIZ-7	**SIV**	Co	3D, 8R × 8R × 8R
Thomsonite	**THO**	Co	3D, 8R × 8R × 8R

[a] Updated based on Table 1 in ref. 8.

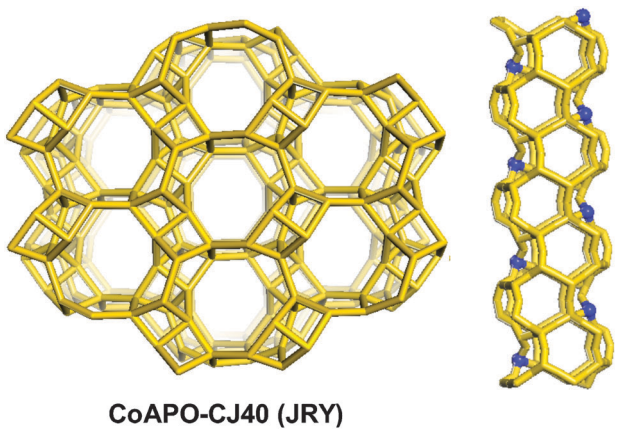

Fig. 12 Framework structure of CoAPO-CJ40 viewed along the [010] direction, and the distribution of Co (blue) atoms in helical 10-ring channels.

3.2 Heteroatom substitution in silicates and germanates

A theoretical study by Brunner and Meier shows that zeolites with low framework density and large micropore volumes could be preferentially formed by small 3-rings and 4-rings.[12] It is known that the T–O bond lengths, especially the T–O–T bond angles will affect the formation of these small rings. In the silicate zeolites, 3-rings and 4-rings are less stable than 5-rings or 6-rings. Compared to the Si–O–Si bond angle, those of Si–O–Ge, Ge–O–Ge, Si–O–Al, and Si–O–B may vary in a relatively small range, which is beneficial for the formation of small rings with high stress. Thus incorporation of heteroatoms in silicates may introduce the possibility of generating new zeolite structures.

The incorporation of Ge atoms into the silicate zeolites has been shown by Corma and coworkers to favour the formation of *d4r* and *d3r* cages, thus leading to novel zeolite structures with low framework density, extra-large pore, and unprecedented pore opening, *etc.* A series of germanosilicate zeolites ITQ-*n* have been discovered coupled with the use of pre-designed organic SDAs in OH^- and F^- in concentrated gels (Table 4). All of these zeolite structures exclusively contain *d4r* cages that are

Table 4 Structural features of germanosilicate ITQ-*n* zeolites[a]

Zeolite	Zeolite type	Building units	Si/Ge ratio	Channel system
ITQ-15	**UTL**	*d4r*	10	2D, 14R × 12R
ITQ-17	**BEC**	*d4r*	2	3D, 12R × 12R × 12R
ITQ-21	—	*d4r*	20	3D, 12R × 12R × 12R
ITQ-22	**IWW**	*d4r*	20	3D, 12R × 10R × 8R
ITQ-24	**IWR**	*d4r*	5	3D, 12R × 10R × 10R
ITQ-26	**IWS**	*d4r*	4	3D, 12R × 12R × 12R
ITQ-29	**LTA**	*d4r*	2	3D, 8R × 8R × 8R
ITQ-33	**ITT**	*d4r*	2	3D, 18R × 10R × 10R
ITQ-34	**ITR**	*d4r*	10	3D, 10R × 10R × 9R
ITQ-37	**-ITV**	*d4r*	1	3D, 30R × 30R × 30R
ITQ-38	**ITG**	*d4r*	4.5	3D, 12R × 10R × 10R
ITQ-40	**-IRY**	*d4r, d3r*	1	3D, 16R × 16R × 15R
ITQ-43	—	*d4r*	2.2	3D, 28R × 12R × 12R
ITQ-44	**IRR**	*d4r, d3r*	2	3D, 18R × 12R × 12R
ITQ-49	**IRN**	*d4r*	4.7	1D, 8R
ITQ-54	—	*d4r*	1	3D, 20R × 14R × 12R

[a] Updated based on the Table 4 in ref. 5.

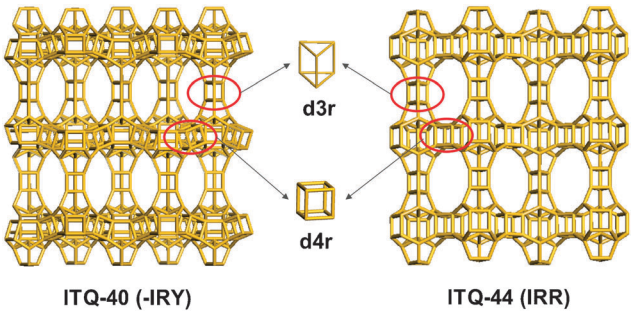

Fig. 13 Framework structures of ITQ-40 and ITQ-44 containing *d3r* and *d4r* cages.

stabilized by the framework Ge atoms and/or the occluded F^- ions. Interestingly, unusual *d3r* cages have been first observed in the germanosilicate zeolite ITQ-40 (**-IRY**).[64] ITQ-40 contains a large 3D channel system and has a low framework-density of 10.1 T/1000 Å^3 (Fig. 13). In its framework, 15-ring channels are running along the [001] direction, which connect to the 2D 16-ring channels running along the ⟨100⟩ directions. The small T–O–T angles (<130°) in *d3r* cages are relaxed by Ge atoms. Besides Ge atoms, Al and B heteroatoms can also be introduced into the framework of ITQ-40.

Another silicogermanate zeolite ITQ-44 (**IRR**) containing *d3r* cages has been synthesized with the directing effect of rigid and bulky SDA **43** and the Ge atoms (Fig. 13).[65] ITQ-44 is the first zeolite possessing a 3D pore system made of intersecting 18- and 12-ring channels. In its framework, Ge atoms preferentially occupy the *d3r* cages (50% occupancy of Ge), then occupy the *d4r* cages (37% occupancy of Ge), indicating the important role of Ge atoms in stabilizing the small *d3r* and *d4r* cages.

On the other hand, the unprecedented pore openings have also been found in germanosilicate zeolites. ITQ-43 is the first hierarchical crystalline zeolite containing 12-ring micropores and 28-ring mesopores in the framework;[19] PKU-16 (**POS**) is the first germanosilicate zeolite with a 3D channel system of 11-rings, 11-rings, and 12-rings;[66] and ITQ-54 is a multi-dimensional extra-large zeolite with 20-ring, 14-ring, and 12-ring pores.[67]

In the reported germanosilicate zeolites, the Si/Ge ratio in the framework varies from 1 to 20. A high content of Ge atoms in the framework may result in a low thermal stability of the product unless the framework density is larger. To meet the practical applications of the germanosilicate zeolites, many attempts have been made to decrease the Ge amount in the framework, and enhance the hydrothermal and thermal stability of the resulting materials. For example, a post synthetic treatment by degradation of zeolite structures through removing Ge-containing *d4r*s, replacing Ge by Si atoms in the framework, post-synthetic isomorphous substitution of Al for Ge, or transformation of the as-synthesized silicogermanate into high-silica zeolitic sheets or related zeolites have been used.[9,10,68] In other way, the suitable SDAs can be designed to better stabilize the structure, thus decreasing the Ge contents in the framework as in the case of pure silica zeolite HPM-1 (**STW**).[48]

Other heteroatoms, such as Zn, Ga, B, Be, Li, *etc.*, can also be incorporated into the zeolite frameworks to form new zeolite structures. Notable examples are zinc-based silicate VPI-9 (**VNI**),[69] gallium-containing silicates TsG-1 (**CGS**)[70] and ECR-34 (**ETR**),[71] borosilicate zeolites SSZ-58 (**SFG**),[72] SSZ-53 (**SFH**),[73] SSZ-60 (**SSY**),[74] and ITQ-52 (**IFW**),[41] beryllosilicate zeolite LSJ-10 (**JOZ**),[75] and Li-containing zeolites **MFI**,[76] **ANA**,[77] RUB-23,[78] and RUB-29,[79] *etc.* ECR-34 is a new gallosilicate zeolite, which possesses 1D extra-large 18-ring channels along the *c*-axis.[71] Notice that no aluminosilicate or silicate analogue of ECR-34 has been found yet. ITQ-52 is synthesized with the organo-phosphorus SDA in the presence of B species.[41] It presents interconnected small and medium pore systems. The as-made ITQ-52 with a Si/B ratio of 17.2 is stable, and most of the B atoms remain in the framework after the removal of organic SDAs upon calcination or thermal treatment under diluted H_2. LSJ-10 (**JOZ**) exhibits the typical framework of beryllosilicate, which features the spiro 5-rings centered on BeO_4 tetrahedra cross-linked by 4- and 5-rings formed from SiO_4 tetrahedra (Fig. 14).[75] It contains 3D 8-ring channels running along *a*, *b*, and *c* axes. LSJ-10 shows high-temperature stability, and its framework remains integrated to 750 °C before starting to recrystallize, which may be related to the small pore structure and strength of the short Be–O and Si–O bonds.

The incorporation of B, Al, and Ga atoms into the germanate frameworks has also been made to synthesize novel zeolite structures. The feasibility of this method is demonstrated by the synthesis of SU-16 (**SOS**), a boron-containing germanate zeolite (Ge/B ratio = 2), under hydrothermal conditions by using SDA **44**.[80] The framework of SU-16 features 3-rings (B_2Ge) and 4-rings (BGe_3). It possesses a 3D intersecting channel system, in which three 8-ring channels and three 12 ring channels are perpendicularly intersected along the [010], [01$\bar{1}$], and [011] directions.

A spiro-5 unit composed of two corner-sharing 3-rings has high inner tension, which is relatively rare in zeolite structures although a few germanate zeolites containing 3-rings have been found. By introducing the Al atom in germanates, a new aluminogermanate zeolite PKU-9 (**PUN**) containing spiro-5 units has been hydrothermally synthesized (Fig. 14).[81] The framework of PKU-9 contains wrinkled CGS layers connected

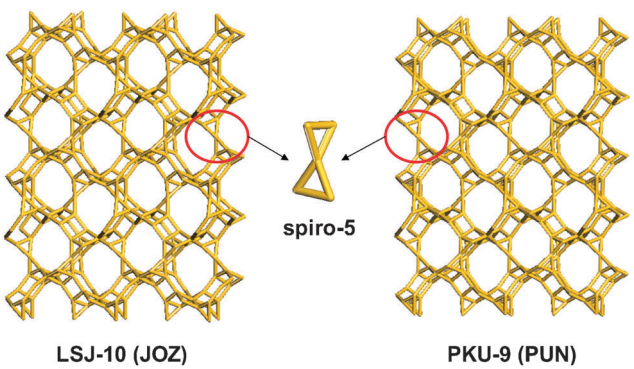

Fig. 14 Framework structures of LSJ-10 and PKU-9 containing spiro-5 units.

by spiro-5 units, which possess 3D channel systems composed of 10-ring channels running along the [001], [110], and [1$\bar{1}$0] directions, and the interconnected 8-ring channels along the [001] direction. Al and Ge atoms are randomly distributed in the framework of PKU-9 with the occupancy of 0.22 and 0.79, respectively. In each spiro-5 unit, the two corner-shared 3-rings are perpendicularly arranged, resulting in the significantly smaller T–O–T angles (123.8–128.9°). The existence of Al atoms may decrease the inner tension of the spiro-5 unit, thus stabilizing the framework structure.

3.3 Heteroatom substitution of oxygen atoms in zeolites

The frameworks of classical zeolites are based on oxide-sharing tetrahedra. The substitution of oxygen by nitrogen in the zeolite frameworks has opened up a new way to synthesize novel zeolite structures that are not feasible as oxides. Nitrido-zeolites are of great interest due to their special chemical and physical properties, such as higher thermal stability and adjustable acidity/basicity. Moreover, nitrogen atoms as three-bridging atoms are commonly found in the framework, and the smaller T–X–T (X = N, O) angles may generate rare 3-rings as well as large rings, forming novel zeolite topologies. Several nitrido-zeolites have been prepared, such as nitridosodalites (**SOD**),[82] related oxonitridosodalites (**SOD**),[83] and nitridophosphate-1 (**NPO**).[84]

Recently, an oxonitridophosphate $Ba_{19}P_{36}O_{6+x}N_{66-x}Cl_{8+x}$ ($x \approx 4.54$) (**NPT**) with novel zeolite topology has been synthesized by heating a reaction mixture of phosphoryl triamide, thiophosphoryl triamide, BaS, and NH_4Cl at 750 °C.[85] Its framework is composed of P(O, N)$_4$ tetrahedra to form a novel $3^8 4^6 8^{12}$ cage. Such cages are further connected to build the framework containing a 3D 8-ring channel system (Fig. 15). The framework of **NPT** has a very high thermal stability up to at least 1100 °C.

Above we have demonstrated the role of heteroatom substitution in directing and stabilizing new zeolite structures. In some heteroatom-containing zeolites with a low degree of substitution, the heteroatoms are randomly distributed in the framework, which may change the framework charge density, but not the framework topology; while in some heteroatom-containing zeolites with a high degree of substitution, the incorporated heteroatoms may change the T–O bond lengths and T–O–T bond angles of TO_4 tetrahedra in the framework, thereby, stabilizing the formation of novel zeolite structures with specific building units. In the latter case, the existence of heteroatom is essential for the synthesis of the specific zeolite structures, in which the heteroatoms may preferentially occupy the special positions in the framework. Notice that a high amount of metal heteroatoms in the framework may decrease the thermal stability of the zeolite. It is important to substitute heteroatoms by Si and/or Al through direct or post-synthesis for their practical applications.

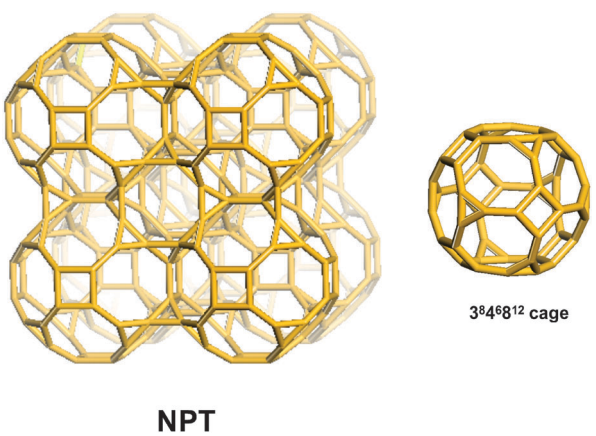

Fig. 15 Framework structure of **NPT** connected by $3^8 4^6 8^{12}$ cages.

4. Zeolites synthesized by topotactic transformation

Different from the traditional synthesis of zeolites under hydrothermal or solvothermal conditions, the topotactic transformation of zeolite frameworks has been developed as an effective method for the synthesis of new zeolite materials. The topotactic transformation of zeolites can be defined as a solid-state structural transformation from one precursor into another structure through a series of treatments, such as dehydration–condensation, intercalation–condensation, degradation–condensation, disassembly–reassembly, and phase-to-phase reconstruction. This method can be used to prepare some new zeolite structures with predetermined layers, cages, and pores. In this section, we will describe the new zeolite structures prepared through the 2D–3D transformation, 3D–2D–3D transformation, and 3D–3D transformation.

4.1 2D–3D transformation

Most of the 2D–3D transformation is the topotactic condensation of the layered precursors into 3D structures by solid-state reaction with thermal treatment. This is a dehydration–condensation process, in which the silanol groups on the surface of two neighboring layers dehydrate and condensate spontaneously, forming high-silica zeolites while keeping the layered structures. In this case, the layer precursor should have the proper number and intra-layer distance of terminal silanol/siloxy groups on either side of the layer, as well as suitable organic SDAs with low charge density.[86] Such a process always leads to guest free materials, which is of particular importance for small pore materials *e.g.* silica sodalite. Also, the platy morphology of the precursor can be maintained.

Early in 1988, Lowe and coworkers reported the synthesis of a thermally stable silica polymorph EU-20 (**CAS**/**NSI**) converted from piperazine silicate EU-19.[87] However, the condensation of EU-19 was only proposed conceptually due to the unclear structure of EU-20. In 1994, boron aluminosilicate zeolite MCM-22 (**MWW**) represented the first example of 2D–3D zeolite transformation, which was synthesized by a layered precursor MCM-22P.[88] Since then, several high-silica zeolites have been prepared by such topotactic conversion of layered silicates (Table 5). Particularly, four new zeolite topologies including

Table 5 Zeolites synthesized by topotactic condensation of layered structures

Type material	Framework type	Precursor
EU-20	**CAS**	EU-19
MCM-22	**MWW**	MCM-22-precursor
RUB-41	**RRO**	RUB-39
RUB-24	**RWR**	R-RUB-18
Zeolite RWR	**RWR**	AA-RUB-18
CDS-1	**CDO**	PLS-1
RUB-37	**CDO**	RUB-36, RUB-38, RUB-48
MCM-65[a]	**CDO**	MCM-65[b]
UZM-25	**CDO**	UZM-13, UZM-17, UZM-19
Unnamed	**CDO**	Several unnamed
Unnamed	**CDO**	PLS-4
RUB-15-SOD	**SOD**	HOAc-RUB-15
Silica-sodalite	**SOD**	HAc-RUB-15
CDS-3	**FER**	PLS-3
Ferrierite	**FER**	PREFER
ERS-12[a]	Incomplete condensation	ERS-12[b]
MCM-47[a]		MCM-47[b]
ERB-1[a]	**MWW**	ERB-1
ITQ-1[a]	**MWW**	ITQ-1[b]
Nu-6(2)	**NSI**	Nu-6(1)
EU-20b	**CAS**	EU-19
IPC-4	**PCR**	IPC-1P

[a] The type material is calcined. [b] The precursor is synthesized without calcination.

CDO, **NSI**, **RRO**, and **RWR** have been discovered, which cannot be obtained by direct hydrothermal synthesis so far.

A silicate zeolite CDS-1 (**CDO**) has been synthesized by dehydration–condensation of layered silicate PLS-1 heated at high temperature under vacuum.[89,90] The sheets of PLS-1 are condensed and polymerized along the [100] direction by dehydration to generate CDS-1, and TMAOH molecules located between the layers are removed. The framework of CDS-1 exhibits a novel zeolite topology, which has straight 8-ring channels along the [010] and [001] directions. The structure of the PLS layer is well maintained in the framework of CDS-1. Other than PLS-1, several layer structures including RUB-36, RUB-38, RUB-48, UZM-13, UZM-17, UZM-19, PSL-4, and MCM-65 have also been used as precursors to prepare CDO-type zeolite structures.

Zanardi *et al.* have studied the transformation of Nu-6(1) and Nu-6(2) (**NSI**), and elucidated their structures using an integrated approach based on experiments and model building.[91] The pentasil layer structure of Nu-6(1) is similar to previously recognized EU-19 and MCM-69, but the SDA of 4,4'-bipyridyne used in the synthesis results in the different symmetry and stacking parameter. The layers of Nu-61 parallel to the (100) plane condense to form a 3D framework of Nu-6(2) with a novel zeolite topology, in which two types of 8-ring channels are found along the *b* direction.

By calcination of a layered silicate RUB-39 at 600 °C, a new high-silica zeolite RUB-41 (**RRO**) with small to medium pores has been obtained.[92] The framework of RUB-41 possesses a 2D channel system with intersecting 8-ring and 10-ring channels running along the [001] and [100] directions, respectively. In addition, a new small pore zeolite RUB-24 (**RWR**) with 1D straight 8-ring channels has also been prepared by topotactic condensation of intercalated silicate layer precursor R-RUB-18 (R = alkylammonium cations) in air at 500 °C.[93]

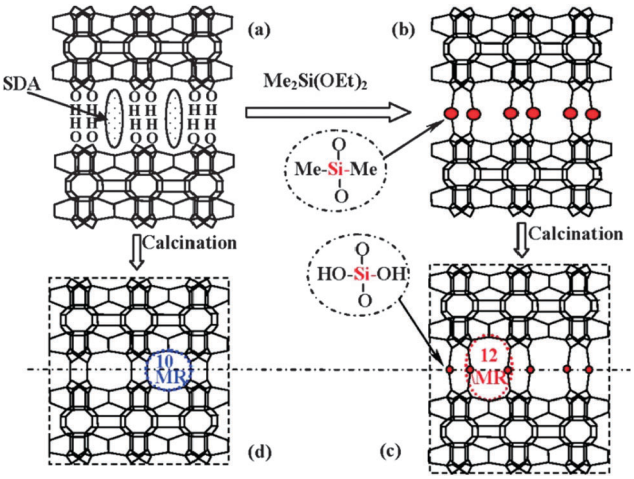

Fig. 16 Post-synthesis of interlayer expanded zeolites through dialkoxysilylation of a lamellar precursor (*e.g.*, MWW precursor): (a) MWW lamellar precursor; (b) interlayer expanded *via* the reaction of silane and silanols; (c) a novel 3D structure with an expanded pore window after calcination, (d) common 3D MWW structure obtained through direct calcination. Reprinted with permission from ref. 94. Copyright 2008 American Chemical Society.

Interestingly, an alternative 2D–3D topotactic transformation has been presented by Wu and coworkers by incorporating Si between layers before condensation.[94] Different from the direct topotactic condensation from layer precursors that generate zeolites with 8-ring or 10-ring pores, such a method may lead to new zeolite structures with more open pores. In their work, one-step post-alkoxysilylation with diethoxydimethylsilane has been realized on the zeolitic lamellar precursors including **MWW**, **FER**, **CDO**, and MCM-47. The new expanded zeolite structures with larger pore windows, high crystallinity, and excellent hydrothermal stability have been obtained by calcination of these post-treated lamellar precursors to remove the organic moieties (Fig. 16). The interlayer-expanded zeolite based on **MWW** precursor exhibits higher catalytic activities in the redox and solid acid-catalyzed reactions of bulky molecules than the conventional **MWW** zeolite. Similar interlayer expansion of the layered zeolite precursors RUB-39 and RUB-36 can yield the new microporous frameworks COE-1/COE-2, and COE-3/COE-4, respectively.[95,96] In addition, a new class of zeolite Lewis acid catalysts can be derived from the layered zeolite precursor RUB-36 by using Fe salt instead of a silylating agent in the interlayer expansion reaction.[97]

In the 2D–3D topotactic transformation, the different condensations of the same layer may give rise to different zeolite structures. For example, the fer layers with an ABAB stacking sequence along the *a*-axis generate zeolites **FER** and **CDO** due to the different shift vector. As for the cas layers, the condensation of cas layers with ABAB and AAAA stacking sequences results in **CAS** and **NSI** zeolite, respectively. Layers A and B are the mirror image of each other.[86]

4.2 3D–2D–3D transformation

Contrast to the 2D–3D topotactic condensation, the 3D–2D–3D framework conversion is also a feasible approach to generate new zeolite structures. The frameworks of some germanosilicate

zeolites are made of 2D layers connected by *d4r* units. Considering that the Ge atoms usually preferentially occupy the *d4r*s, and the bond between the layers and *d4r*s is easy to hydrolyse in the presence of water, the 3D–2D conversion can be achieved by degradation of interlayer *d4r* connectors. The resulting 2D layers are further condensed by calcination to form a novel 3D zeolite structure. This topotactic condensation can decrease the Ge contents in the framework, as well as synthesize new zeolite structures.

A successful example of 3D–2D–3D transformation is presented by Cějka and coworkers.[98] In detail, the calcined **UTL** zeolite as a precursor is treated hydrothermally from room temperature to 100 °C and the pH range is adjusted from neutral to acidic (0.1 M HCl). The *d4r* units are removed from the structure, resulting in the transformation of the 3D structure into the 2D lamellar layer (denoted IPC-1P). Then, the new IPC-1P layers are further modified with a silylating agent in the nitric acid solution, and generating new germanosilicate zeolite IPC-2 (**OKO**) after calcination. Another example of 3D–2D–3D conversion is achieved by Kirschhock and coworkers in the transformation of IM-12 (**UTL**) zeolite into a new Ge-free zeolite COK-14 (**OKO**).[99] Ge-containing *d4r* units in the germanosilicate IM-12 can be removed in strong mineral acid. By leaching and calcination of the products, the new all-silica zeolite COK-14 with an intersecting 12- and 10-ring channel system is prepared.

Remarkably, a top-down method has been developed by Cějka and coworkers, which involves the disassembly of a parent zeolite into its constituent layers followed by their reassembly into new zeolites with targeted topologies.[100] The idea of this method is tailoring the linkers used in the reassembly, and further to control the generated structures with predetermined pore sizes. Two new zeolites IPC-4 (**PCR**) and IPC-2 (**OKO**) have been synthesized by using this strategy from a parent zeolite **UTL** with 12-ring and 14-ring channels. The replacement of *d4r*s in **UTL** by 4-rings or oxygen atoms results in IPC-2 with smaller 12 × 10 ring channels and IPC-4 with even smaller 10 × 8 ring channels, respectively. Note that there is no direct synthesis route available yet for IPC-2 and IPC-4 zeolites.

Recently, the mechanism of the disassembly and reassembly of the layered silicate precursor RUB-36 to FER-type zeolite has been studied.[101] This opens up new vistas for the synthesis of new zeolite structures through topotactic transformations.

4.3 3D–3D reconstructive transformation

More recently, an interesting 3D–3D reconstructive transformation of zeolite through the effect of pressure has been shown, and a new zeolite ITQ-50 (**IFY**) was produced from the pure silica zeolite ITQ-29 (**LTA**).[102] ITQ-29 undergoes two structural transformations under pressure. A reversible transformation occurs at 1.2 GPa and ITQ-29 is recovered after pressure release. Moreover, an order-to-order reconstructive phase transition occurs at approximately 3.2 GPa, leading to a new crystalline zeolite ITQ-50 (**IFY**) that is non-reversible upon pressure release. The structures of ITQ-29 and ITQ-50 are quite different although some of their building units are related. The framework of ITQ-29 is composed of three composite building units (CBUs) including *lta*, *sod*, and *d4r*. During the phase transition of ITQ-29 to ITQ-50, *lta* cages change to *ify* cages, half of the *d4r* cages remain and the others convert to *sti* units through the breakage of one edge of *d4r* cages, and the *sod* cages are kept. As a result, ITQ-50 possesses 2D interconnected 8-ring channels along the [001] and [110] directions. Fig. 17 shows the transformation of *lta* cages into *ify* cages through three structural modifications.

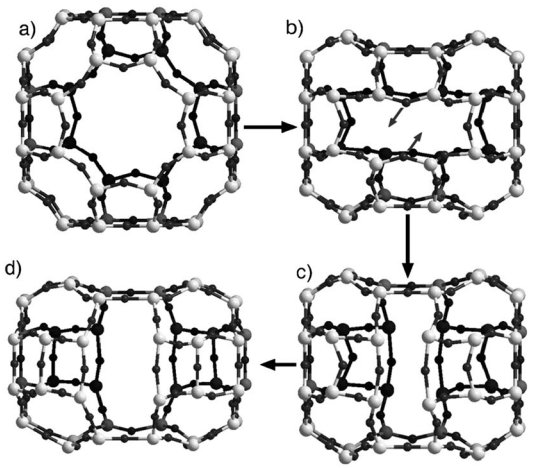

Fig. 17 Suggested pathway from ITQ-29 to ITQ-50. (a to b) Reversible deformation; (b to c) Si–O bond breaking and formation through displacement of O atoms; (c to d) structure relaxation. Reprinted with permission from ref. 102. Copyright 2013 Wiley-VCH.

To date, new zeolites obtained through the topotactic transformation have been relatively rare. Synthesis of novel and thermally stable layered zeolite precursors by the direct synthesis or post-synthesis treatments is the key for this strategy. In addition, exploitation of more feasible methods to achieve the effective topotactic transformation, as well as the understanding of their transformation mechanisms may allow us to prepare many more novel zeolite structures.

5. Summary and perspectives

The number of new zeolite structures has been rapidly growing in the last decade. Since porous materials are involved in various processes of current interest, energy saving catalytic processes, environmentally benign sorbents, storage materials for waste and energy *etc.*, in general, there is potential in every new material synthesized. In this review, we have demonstrated the recent progress achieved in the synthesis of new zeolite structures by applying the three main synthetic strategies based on pre-designed organic SDAs, heteroatom substitution, and topotactic transformation. Utilization of pre-designed organic SDAs allows the synthesis of new zeolites with hierarchical pores, odd-rings, extra-large pores, and extremely complex framework topologies, *etc.*; utilization of heteroatom substitution allows the synthesis of new zeolites with low framework density, extra-large pores, chiral pores, and special building units (*d3r*, *d4r*, 3-rings, 4-rings, *etc.*); utilization of topotactic transformation allows the synthesis of new zeolites with predetermined layers, pores, and cages. The discovery of these new zeolites with unprecedented structural features may offer new

perspectives for zeolite materials in applications in catalysis and adsorption–separation.

Despite the synthesis progress made, several challenges remain in the synthesis of new zeolite materials. The first one is the synthesis of zeolites with extra-large pores/cavities and high thermal stability for the application in catalysis of heavy oils. This needs the design of novel SDAs (*e.g.*, bulky and rigid SDAs, supramolecular organic SDAs, *etc.*) and increasing the Si contents in the framework. Second is the discovery of new zeolites with special pore rings, such as 11-, 13-, 15-, 17-, and 19-rings, which could be useful for shape-selective catalysis. For doing this it is possible to theoretically predict such zeolite structures, and then design organic SDAs and select framework cations to direct their synthesis. Third is the synthesis of a single enantiomer of a chiral zeolite for the applications in asymmetric catalysis and separations. For this purpose, efforts should be devoted to the following aspects: (1) selecting suitable framework atoms to favour the formation of a chiral framework; (2) using chiral SDAs (*e.g.*, metal complexes) to direct the chiral structure units and further organize the chiral framework; (3) attaching the chiral molecules or groups (*e.g.*, chiral organosilane) to the inorganic framework through covalent bonds during the nucleation process to generate chiral structures.

Currently, the rapidly developed computation techniques play an important role in the prediction of hypothetical zeolite structures.[12] A large number of hypothetical zeolites with desired pore architectures have been designed.[103,104] Towards the rational synthesis of target hypothetical zeolites,[5,6] the suitable SDA candidates should be predicted by using the computational modeling or the "*ab initio*" design, followed by the proper selection of the framework cations based on their structural features. Data mining techniques and various synthetic approaches (particularly high throughput techniques) will greatly guide their synthesis by predicting the synthesis conditions and fast-screening the experiments. The computational chemistry has become a very important tool in assisting the discovery of new zeolites. It is worth noting that a deep understanding of the formation mechanism at the molecular level is essential for the rationalization of zeolite synthesis. Moreover, the spirit of the chemists is the driving force leading us to promoting the development of zeolite science in the near future. We hope that this view will stimulate more advances in the synthesis of new zeolites with predetermined structures and functions.

Abbreviations

The full names for SDAs (only one name is given for a complicated SDA):

1 1-Butyl-1-cyclohexylpyrrolidinium;
2 1-Cyclohexyl-1-methylpyrrolidinium;
3 1-Cyclohexyl-1-ethylpyrrolidinium;
4 1-Butyl-1-cyclooctylpyrrolidinium;
5 1-Butyl-1-cyclooctyl-3-methylpyrrolidinium;
6 (2′*R*,6′*S*)-2′,6′-Dimethylspiro[isoindoline-2,1′-piperidin]-1′-ium hydroxide;
7 (1*S*,6*S*)-2,2-Diethyl-6,7-dimethyl-2-azoniabicyclo[3.2.2]-nonane;
8 18-Azonia-8,8-diethyltetracyclo[4.3.3.1^{2,5}.0^{1,6}]tridec-3-ene;
9 1,1′-(Hexane-1,6-diyl)bis(1-methylpyrrolidinium);
10 1′-(Pentane-1,5-diyl)bis(1-methylpyrrolidinium);
11 1,1′-(Butane-1,4-diyl)bis(1-methylpyrrolidinium);
12 1,6-Bis(*N*-cyclohexylpyrrolidinium)hexane;
13 N^1,N^1,N^1,N^3,N^3,N^3-Hexamethylpropane-1,3-diaminium;
14 N^1,N^1,N^1,N^4,N^4,N^4-Hexamethylbutane-1,4-diaminium;
15 N^1,N^1,N^1,N^5,N^5,N^5-Hexamethylpentane-1,5-diaminium;
16 Decamethonium;
17 N^1,N^1,N^1,N^6,N^6,N^6-Hexamethylhexane-1,6-diaminium;
18 *N*,*N*,*N*′,*N*′-Tetraethyl-1,8-dimethyl-bicyclo-*exo*,*exo*-[2.2.2]oct-7-ene-2,3:5,6-dipyrrolidinium;
19 3′,4′-Dihydro-1′*H*-spiro[isoindoline-2,2′-isoquinolin]-2-ium;
20 1,1-Dipropyl-4-(1-propylpyrrolidinium-1-yl)piperidinium;
21 (1,3-Phenylenebis(methylene))bis(triethylphosphonium);
22 Dimethyldiphenylphosphonium;
23 Hexane-1,6-bis(trimethylammonium);
24 Propane-1,3-diylbis(trimethylphosphonium);
25 Propane-1,3-diylbis(trimethylphosphonium);
26 Butane-1,4-diylbis(tri-*tert*-butylphosphonium);
27 3,3,8,8-Tetrakis(dimethylamino)-2,9-dimethyl-2,9-diaza-3,8-diphosphoniadecane-3,8-diium;
28 *tert*-Butyl-iminotris(dimethylamino)phosphorane;
29 1,8-Bis(dimethylamino)naphthalene;
30 1-Ethyl-3-methyl-1*H*-imidazol-3-ium;
31 1-Butyl-3-methyl-1*H*-imidazol-3-ium;
32 2-Ethyl-1,3,4-trimethyl-1*H*-imidazol-3-ium;
33 1-Methyl-3-(4-methylbenzyl)-1*H*-imidazol-3-ium;
34 1-Methyl-3-(naphthalen-2-ylmethyl)-1*H*-imidazol-3-ium;
35 Bis(tetramethylcyclopentadienyl)cobalt(III);
36 Bis(pentamethylcyclopentadienyl)cobalt(III);
37 $[Ni(en)_3]^{2+}$ (en = ethylenediamine);
38 $[Ni(1,2\text{-PDA})_3]^{2+}$ (1,2-PDA = 1,2-diaminopropane);
39 *N*-Methylpiperazine;
40 Diethylamine;
41 Diethyldimethylammonium;
42 Ethyltrimethylammonium;
43 (2′-(*R*),6′-(*S*))-2′,6′-Dimethylspiro[isoindole-2,1′-piperidin-1′-ium];
44 Diethylenetriamine

Acknowledgements

We thank the State Basic Research Project of China (Grant no. 2011CB808703 and 2014CB931802) and the National Natural Science Foundation of China (Grant no. 21271081, 91122029 and 21320102001) for financial supports.

References

1 J. Čejka, A. Corma and S. Zones, *Zeolites and Catalysis: Synthesis Reactions and Applications*, Wiley, Weinheim, 2010.
2 M. E. Davis, *Nature*, 2002, **417**, 813–821.

3 R. M. Barrer, *J. Chem. Soc.*, 1948, 127–132.
4 C. S. Cundy and P. A. Cox, *Microporous Mesoporous Mater.*, 2005, **82**, 1–78.
5 Z. Wang, J. Yu and R. Xu, *Chem. Soc. Rev.*, 2012, **41**, 1729–1741.
6 J. Yu and R. Xu, *Acc. Chem. Res.*, 2010, **43**, 1195–1204.
7 M. Moliner, F. Rey and A. Corma, *Angew. Chem., Int. Ed.*, 2013, **52**, 13880–13889.
8 J. Li, J. Yu and R. Xu, *Proc. R. Soc. A*, 2012, **468**, 1955–1967.
9 W. J. Roth, P. Nachtigall, R. E. Morris and J. Čejka, *Chem. Rev.*, 2014, **114**, 4807–4837.
10 U. Díaz and A. Corma, *Dalton Trans.*, 2014, **43**, 10292–10316.
11 M. B. Park, S. J. Cho and S. B. Hong, *J. Am. Chem. Soc.*, 2011, **133**, 1917–1934.
12 Y. Li and J. Yu, *Chem. Rev.*, 2014, **114**, 7268–7316.
13 C. Baerlocher and L. B. McCusker, Database of Zeolite Structures, http://www.iza-structure.org/databases/.
14 J. Jiang, J. Yu and A. Corma, *Angew. Chem., Int. Ed.*, 2010, **49**, 3120–3145.
15 S. Elomari, *US Pat.*, 6 616 911, 2003.
16 S. Elomari, *US Pat.*, 6 544 495, 2003.
17 C. Baerlocher, T. Weber, L. B. McCusker, L. Palatinus and S. I. Zones, *Science*, 2011, **333**, 1134–1137.
18 A. Burton, S. Elomari, R. C. Medrud, I. Y. Chan, C. Y. Chen, L. M. Bull and E. S. Vittoratos, *J. Am. Chem. Soc.*, 2003, **125**, 1633–1642.
19 J. Jiang, J. L. Jordá, J. Yu, L. A. Baumes, E. Mugnaioli, M. J. Díaz-Cabañas, U. Kolb and A. Corma, *Science*, 2011, **333**, 1131–1134.
20 J. Jiang, Y. Xu, P. Cheng, Q. Sun, J. Yu, A. Corma and R. Xu, *Chem. Mater.*, 2011, **23**, 4709–4715.
21 D. Xie, L. B. McCusker, C. Baerlocher, S. I. Zones, W. Wan and X. Zou, *J. Am. Chem. Soc.*, 2013, **135**, 10519–10524.
22 S. Smeets, D. Xie, C. Baerlocher, L. B. McCusker, W. Wan, X. Zou and S. I. Zones, *Angew. Chem., Int. Ed.*, 2014, **53**, 10398–10402.
23 S. Elomari, A. W. Burton, K. Ong, A. R. Pradhan and I. Y. Chan, *Chem. Mater.*, 2007, **19**, 5485–5492.
24 S. I. Zones, A. W. Burton and K. Ong, *International Pat.*, WO 2007/079038, 2007.
25 E. Benazz, J. L. Guth and L. Rouleau, *Patent Cooperation Treaty*, WO 98/17581, 1998.
26 S. B. Hong, E. G. Lear, P. A. Wright, W. Zhou, P. A. Cox, C. H. Shin, J. H. Park and I. S. Nam, *J. Am. Chem. Soc.*, 2004, **126**, 5817–5826.
27 A. Jackowski, S. I. Zones, S. J. Hwang and A. W. Burton, *J. Am. Chem. Soc.*, 2009, **131**, 1092–1100.
28 A. W. Burton, *US Pat.*, 7 820 141, 2010.
29 Y. Lorgouilloux, M. Dodin, E. Mugnaioli, C. Marichal, P. Caullet, N. Bats, U. Kolb and J. Paillaud, *RSC Adv.*, 2014, **4**, 19440–19449.
30 M. Afeworki, D. L. Dorset, G. J. Kennedy and K. G. Strohmaire, *Chem. Mater.*, 2006, **18**, 1697–1704.
31 J. Sun, C. Bonneau, Á. Cantín, A. Corma, M. J. Díaz-Cabañas, M. Moliner, D. Zhang, M. Li and X. Zou, *Nature*, 2009, **458**, 1154–1157.
32 K. Qian, J. Li, J. Jiang, Z. Liang, J. Yu and R. Xu, *Microporous Mesoporous Mater.*, 2012, **164**, 88–92.
33 M. Moliner, J. González, M. T. Portilla, T. Willhammar, F. Rey, F. J. Llopis, X. Zou and A. Corma, *J. Am. Chem. Soc.*, 2011, **133**, 9497–9505.
34 T. Willhammar, J. Sun, W. Wan, P. Olevnikov, D. Zhang, X. Zou, M. Moliner, J. Gonzalez, C. Martínez, F. Rey and A. Corma, *Nat. Chem.*, 2012, **4**, 188–194.
35 M. Moliner, T. Willhammar, W. Wan, J. González, F. Rey, J. L. Jorda, X. Zou and A. Corma, *J. Am. Chem. Soc.*, 2012, **134**, 6473–6478.
36 D. L. Dorset, K. G. Strohmaier, C. E. Kliewer, A. Corma, M. J. Díaz-Cabañas, F. Rey and C. J. Gilmore, *Chem. Mater.*, 2008, **20**, 5325–5331.
37 D. L. Dorset, G. J. Kennedy, K. G. Strohmaier, M. J. Díaz-Cabañas, F. Rey and A. Corma, *J. Am. Chem. Soc.*, 2006, **128**, 8862–8867.
38 A. Corma, M. J. Díaz-Cabañas, J. L. Jordá, F. Rey, G. Sastre and K. G. Strohmaier, *J. Am. Chem. Soc.*, 2008, **130**, 16482–16483.
39 T. Boix, M. Puche, M. A. Camblor and A. Corma, *US Pat.*, 6 471 941, 2002.
40 M. Hernández-Rodríguez, J. L. Jordá, F. Rey and A. Corma, *J. Am. Chem. Soc.*, 2012, **134**, 13232–13235.
41 R. Simancas, J. L. Jordá, F. Rey, A. Corma, A. Cantín, I. Peral and C. Popescu, *J. Am. Chem. Soc.*, 2014, **136**, 3342–3345.
42 R. Martínez-Franco, M. Moliner, Y. Yun, J. Sun, W. Wan, X. Zou and A. Corma, *Proc. Natl. Acad. Sci. U. S. A.*, 2013, **110**, 3749–3754.
43 S. I. Zones, *Zeolites*, 1989, **9**, 458–467.
44 P. A. Barrett, T. Boix, M. Puche, D. H. Olson, E. Jordan, H. Köller and M. A. Camblor, *Chem. Commun.*, 2003, 2114–2115.
45 Y. Lorgouilloux, M. Dodin, J. L. Paillaud, P. Caullet, L. Michelin, L. Josien, O. Ersen and N. Bats, *J. Solid State Chem.*, 2009, **182**, 622–629.
46 M. Dodin, J.-L. Paillaud, Y. Lorgouilloux, P. Caullet, E. Elkaïm and N. Bats, *J. Am. Chem. Soc.*, 2010, **132**, 10221–10223.
47 L. Tang, L. Shi, C. Bonneau, J. Sun, H. Yue, A. Ojuva, B. L. Lee, M. Kritikos, R. G. Bell, Z. Bacsik, J. Mink and X. Zou, *Nat. Mater.*, 2008, **7**, 381–385.
48 A. Rojas and M. A. Camblor, *Angew. Chem., Int. Ed.*, 2012, **51**, 3854–3856.
49 A. Corma, F. Rey, J. Rius, M. J. Sabater and S. Valencia, *Nature*, 2004, **431**, 287–290.
50 F. Chen, Y. Xu and H. Du, *Angew. Chem., Int. Ed.*, 2014, **53**, 9592–9596.
51 K. J. Balkus and A. G. Gabrielov Jr., *US Pat.*, 5 489 424, 1996.
52 Y. Han, Y. Li, J. Yu and R. Xu, *Angew. Chem., Int. Ed.*, 2011, **50**, 3003–3005.
53 Y. Xu, Y. Li, Y. Han, X. Song and J. Yu, *Angew. Chem., Int. Ed.*, 2013, **52**, 5501–5503.
54 R. Martínez-Franco, M. Moliner, C. Franch, A. Kustov and A. Corma, *Appl. Catal., B*, 2012, **127**, 273–280.
55 R. Martínez-Franco, M. Moliner, J. R. Thogersen and A. Corma, *ChemCatChem*, 2013, **5**, 3316–3323.
56 R. Martínez-Franco, M. Moliner, P. Concepcion, J. R. Thogersen and A. Corma, *J. Catal.*, 2014, **314**, 73–82.

57 R. Martínez-Franco, M. Moliner and A. Corma, *J. Catal.*, 2014, **319**, 36–43.
58 L. Ren, L. Zhu, C. Yang, Y. Chen, Q. Sun, H. Zhang, C. Li, F. Nawaz, X. Meng and F. Xiao, *Chem. Commun.*, 2011, **47**, 9789–9791.
59 Y. Li, J. Yu and R. Xu, *Angew. Chem., Int. Ed.*, 2013, **52**, 1673–1677.
60 X. Song, Y. Li, L. Gan, Z. Wang, J. Yu and R. Xu, *Angew. Chem., Int. Ed.*, 2009, **48**, 314–317.
61 Z. Liu, X. Song, J. Li, Y. Li, J. Yu and R. Xu, *Inorg. Chem.*, 2012, **51**, 1969–1974.
62 L. Shao, Y. Li, J. Yu and R. Xu, *Inorg. Chem.*, 2012, **51**, 225–229.
63 R. W. Broach, N. Greenlay, P. Jakubczak, L. M. Knight, S. R. Miller, J. P. S. Mowat, J. Stanczyk and G. J. Lewis, *Microporous Mesoporous Mater.*, 2014, **189**, 49–63.
64 A. Corma, M. J. Díaz-Cabañas, J. Jiang, M. Afeworki, D. L. Dorset, S. L. Soled and K. G. Strohmaier, *Proc. Natl. Acad. Sci. U. S. A.*, 2010, **107**, 13997–14002.
65 J. Jiang, J. L. Jordá, M. J. Díaz-Cabañas, J. Yu and A. Corma, *Angew. Chem., Int. Ed.*, 2010, **49**, 4986–4988.
66 W. Hua, H. Chen, Z. Yu, X. Zou, J. Lin and J. Sun, *Angew. Chem., Int. Ed.*, 2014, **53**, 5868–5871.
67 J. Jiang, Y. Yun, X. Zou, J. L. Jordá and A. Corma, *Chem. Sci.*, 2015, **6**, 480–485.
68 F. Gao, M. Jaber, K. Bozhilov, A. Vicente, C. Fernandez and V. Valtchev, *J. Am. Chem. Soc.*, 2009, **131**, 16580–16586.
69 L. B. McCusker, R. W. Grosse-Kunstleve, C. Baerlocher, M. Yoshikawa and M. E. Davis, *Microporous Mater.*, 1996, **6**, 295–309.
70 Y. Lee, S. J. Kim, G. Wu and J. B. Parise, *Chem. Mater.*, 1999, **11**, 879–881.
71 K. G. Strohmaier and D. E. W. Vaughan, *J. Am. Chem. Soc.*, 2003, **125**, 16035–16039.
72 A. Burton, S. Elomari, R. C. Medrud, I. Y. Chan, C. Y. Chen, L. M. Bull and E. S. Vittoratos, *J. Am. Chem. Soc.*, 2003, **125**, 1633–1642.
73 A. Burton, S. Elomari, C.-Y. Chen, R. C. Medrud, I. Y. Chan, L. M. Bull, C. Kibby, T. V. Harris, S. I. Zone and E. S. Vittoratos, *Chem. – Eur. J.*, 2003, **9**, 5737–5748.
74 A. Burton and S. Elomari, *Chem. Commun.*, 2004, 2618–2619.
75 J. A. Armstrong and M. T. Weller, *J. Am. Chem. Soc.*, 2010, **132**, 15679–15686.
76 S. H. Park, H. Liu, M. Kleinsorge, C. P. Grey, B. H. Toby and J. B. Parise, *Chem. Mater.*, 2004, **16**, 2605–2614.
77 S. H. Park, H. Gies, B. H. Toby and J. B. Parise, *Chem. Mater.*, 2002, **14**, 3187–3196.
78 S. H. Park, P. Daniels and H. Gies, *Microporous Mesoporous Mater.*, 2000, **37**, 129–143.
79 S. H. Park, J. B. Parise, H. Gies, H. Liu, C. P. Gery and B. H. Toby, *J. Am. Chem. Soc.*, 2000, **122**, 11023–11024.
80 Y. Li and X. Zou, *Angew. Chem., Int. Ed.*, 2005, **44**, 2012–2015.
81 J. Su, Y. Wang, Z. Wang and J. Lin, *J. Am. Chem. Soc.*, 2009, **131**, 6080–6081.
82 W. Schnick and J. Lücke, *Angew. Chem., Int. Ed.*, 1992, **31**, 213–215.
83 N. Stock, E. Irran and W. Schnick, *Chem. – Eur. J.*, 1998, **4**, 1822–1828.
84 S. Correll, O. Oeckler, N. Stock and W. Schnick, *Angew. Chem., Int. Ed.*, 2003, **42**, 3549–3552.
85 S. J. Sedlmaier, M. Döblinger, O. Oeckler, J. Weber, J. Schmedt auf der Günne and W. Schnick, *J. Am. Chem. Soc.*, 2011, **133**, 12069–12078.
86 B. Marler and H. Gies, *Eur. J. Mineral.*, 2012, **24**, 405–428.
87 A. J. Blake, K. R. Franklin and B. M. Lowe, *J. Chem. Soc., Dalton Trans.*, 1988, 2513–2517.
88 M. E. Leonowicz, J. A. Lawton, S. L. Lawton and M. K. Rubin, *Science*, 1994, **264**, 1910–1913.
89 T. Ikeda, Y. Akiyama, Y. Oumi, A. Kawai and F. Mizukami, *Angew. Chem., Int. Ed.*, 2004, **43**, 4892–4896.
90 B. Marler, Y. Wang, J. Song and H. Gies, *Dalton Trans.*, 2014, **43**, 10396–10416.
91 S. Zanardi, A. Alberti, G. Cruciani, A. Corma, V. Fornés and M. Brunelli, *Angew. Chem., Int. Ed.*, 2004, **43**, 4933–4937.
92 Y. X. Wang, H. Gies, B. Marler and U. Müller, *Chem. Mater.*, 2005, **17**, 43–49.
93 B. Marler, N. Ströter and H. Gies, *Microporous Mesoporous Mater.*, 2005, **83**, 201–211.
94 P. Wu, J. Ruan, L. Wang, L. Wu, Y. Wang, Y. Liu, W. Fan, M. He, O. Terasaki and T. Tatsumi, *J. Am. Chem. Soc.*, 2008, **130**, 8178–8187.
95 H. Gies, U. Müller, B. Yilmaz, T. Tatsumi, B. Xie, F. Xiao, X. Bao, W. Zhang and D. D. Vos, *Chem. Mater.*, 2011, **23**, 2545–2554.
96 H. Gies, U. Müller, B. Yilmaz, M. Feyen, T. Tatsumi, H. Imai, W. Zhang, B. Xie, F. Xiao, X. Bao, W. Zhang, T. D. Baerdemaeker and D. D. Vos, *Chem. Mater.*, 2012, **24**, 1536–1545.
97 T. D. Baerdemaeker, H. Gies, B. Yilmaz, U. Müller, M. Feyen, F. Xiao, W. Zhang, T. Yokoi, X. Bao and D. D. Vos, *J. Mater. Chem. A*, 2014, **2**, 9709–9717.
98 W. J. Roth, O. V. Shvets, M. Shamzhy, P. Chlubná, M. Kubù, P. Nachtigall and J. Èejka, *J. Am. Chem. Soc.*, 2011, **133**, 6130–6133.
99 E. Verheyen, L. Joos, K. Van Havenbergh, E. Breynaert, N. Kasian, E. Gobechiya, K. Houthoofd, C. Martineau, M. Hinterstein, F. Taulelle, V. V. Speybroeck, M. Waroquier, S. Bals, G. Van Tendeloo, C. E. A. Kirschhock and J. A. Martens, *Nat. Mater.*, 2012, **11**, 1059–1064.
100 W. J. Roth, P. Nachtigall, R. E. Morris, P. S. Wheatley, V. R. Seymour, S. E. Ashbrook, P. Chlubná, L. Grajciar, M. Položij, A. Zukal, O. Shvets and J. Èejka, *Nat. Chem.*, 2013, **5**, 628–633.
101 Z. Zhao, W. Zhang, P. Ren, W. Han, U. Müller, B. Yilmaz, M. Feyen, H. Gis, F. Xiao, D. D. Vos, T. Tatsumi and X. Bao, *Chem. Mater.*, 2013, **25**, 840–847.
102 J. L. Jordá, F. Rey, G. Sastre, S. Valencia, M. Palomino, A. Corma, A. Segura, D. Errandonea, R. Lacomba, F. J. Manjón, O. Gomis, A. K. Kleppe, A. P. Jephcoat, M. Amboage and J. A. Rodríguez-Velamazán, *Angew. Chem., Int. Ed.*, 2013, **52**, 10458–10462.
103 M. D. Foster and M. M. J. Treacy, A Database of Hypothetical Zeolite Structures, http://www.hypotheticalzeolites.net.
104 Y. Li, J. Yu and R. Xu, Hypothetical Zeolite Database, http://mezeopor.jlu.edu.cn/hypo.